Symbolic recursion method for strongly correlated fermions in two and three dimensions

Igor Ermakov[1, 2, 3, *] and Oleg Lychkovskiy[4, 3, †]

[1] *Wilczek Quantum Center, Shanghai Institute for Advanced Studies,*
University of Science and Technology of China, Shanghai 201315, China
[2] *Hefei National Laboratory, Hefei 230088, China*
[3] *Department of Mathematical Methods for Quantum Technologies,*
Steklov Mathematical Institute of Russian Academy of Sciences, 8 Gubkina St., Moscow 119991, Russia.
[4] *Skolkovo Institute of Science and Technology, Bolshoy Boulevard 30, bld. 1, Moscow 121205, Russia.*

(Dated: January 28, 2026)

We present a symbolic implementation of the recursion method for the real-time dynamics of strongly correlated fermions on one-, two- and three-dimensional lattices. Focusing on two paradigmatic models – interacting spinless fermions and the Hubbard model – we find that the behavior of Lanczos coefficients is compatible with the universal operator growth hypothesis, exhibiting an approximately linear growth. Leveraging symbolically computed Lanczos coefficients and their asymptotic behavior, we access infinite-temperature autocorrelation functions up to times sufficient for thermalization to occur, directly in the thermodynamic limit. This, in turn, unlocks transport properties. In particular, we compute with high precision the charge diffusion constant over a broad range of interaction strengths, V. Surprisingly, the results are well described by a simple functional dependence $\sim 1/V^2$, which holds universally both for small and large V. Our results highlight the promise of a symbolic computational paradigm in which the most computationally expensive step is performed once, yielding reusable symbolic output that enables efficient evaluation of physical observables for arbitrary model parameters.

Dynamics and transport in strongly correlated electron systems, such as the spinless-fermion t-V model and the Hubbard model, have been at the forefront of condensed-matter physics for decades [1–9]. Accurate simulation of these models remains one of the central challenges of modern theoretical physics. Approaches based on the direct diagonalization of Hamiltonians are fundamentally limited by the exponential growth of the many-body Hilbert space with the system size [10, 11]. In one dimension, remarkable progress has been achieved using integrability-based techniques [12, 13] and tensor-network methods [14], to the point that a broad class of dynamical and transport problems, with certain reservations, can now be considered simulable in 1D. In higher dimensions the substantial progress has been achieved using a variety of analytical and numerical approaches [9, 15–28]. In parallel, considerable efforts have focused on quantum simulation platforms, which aim to realize synthetic correlated many-body systems and probe their properties experimentally [29–33]. Despite impressive recent progress, such platforms remain at an early stage of development and would greatly benefit from reliable computational benchmarks capable of guiding both experiments and theory.

In this work, we develop a symbolic computational approach to the dynamics of strongly correlated fermionic systems based on the recursion method. While first introduced decades ago [34–38], the recursion method has seen renewed attention due to recent theoretical progress on operator growth [39–48] and the increase of computational capabilities.

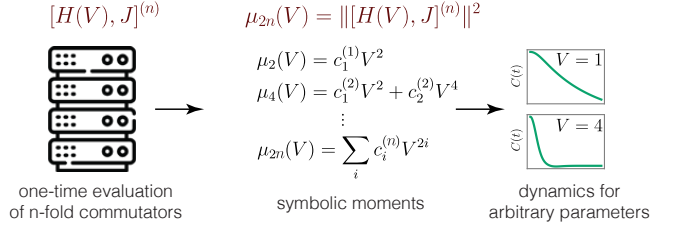The recursion method has been successfully applied in

FIG. 1. Reusable symbolic computation workflow: the computationally expensive symbolic evaluation of the n-fold commutators $[H(V), A]^{(n)}$ is carried out once, while the resulting symbolic moments $\mu_{2n}(V)$ are subsequently reused multiple times to compute correlation functions $C(t)$ at specific values of the parameter V.

a variety of settings, including interacting spin-1/2 systems [49–55] and higher-spin models [56]. Other methods to address quantum many-body dynamics in Heisenberg representation have also emerged [57–63], typically formulated within qubit operator spaces where the Pauli-string basis provides a natural framework.

Fermionic models pose additional challenges. In Monte Carlo methods, these challenges manifest themselves as the infamous sign problem. In operator-based approaches, difficulties arise from the anticommutation relations of fermionic operators on spatially separated sites.

We report the successful application of the advanced recursion method to interacting fermionic systems on one-, two-, and three-dimensional lattices. In one dimension, the recursion method is known to be less efficient than state-of-the-art approaches based on exact

diagonalization or matrix product states [52, 55, 64]. For this reason, applying the recursion method in one dimension serves the sole purpose of cross-checking its results against those from exact diagonalization. In contrast, real-time dynamics in two and three spatial dimensions is widely believed to be challenging for established numerical methods. We demonstrate that the advanced recursion method is a powerful technique applicable in higher dimensions, capable of capturing the dynamics over the entire time domain – from short times to thermalization – in the strongly correlated regime and without finite-size effects.

The rest of the manuscript is organized as follows. In the next section, we introduce specific models under study. Then we discuss the autocorrelation function and its moments. After that, we briefly review the recursion method and the universal operator growth hypothesis (UOGH) [41], present Lanczos coefficients for interacting fermionic models and demonstrate that they are compatible with the UOGH. Subsequently, we present infinite-temperature autocorrelation functions obtained from the recursion method supplemented by the UOGH. Then we apply the recursion method to describe transport in the models under study. Specifically, we compute the diffusion constant and the conductivity for a broad range of interaction strengths. In the End Matter, we describe important details of the algorithm and software implementation. Further details are relegated to the Supplemental Material [65].

Models and observables. We consider two fermionic models on hypercubic lattices. The first one is the spinless fermion t-V model,

$$H_{tV} = -t_{\mathrm{hop}} \sum_{\langle i,j \rangle} \left(c_i^\dagger c_j + \mathrm{H.c.} \right) + V \sum_{\langle i,j \rangle} \left(n_i - \tfrac{1}{2} \right)\left(n_j - \tfrac{1}{2} \right). \tag{1}$$

The second one is the Hubbard model,

$$H_{\mathrm{Hub}} = -t_{\mathrm{hop}} \sum_{\langle i,j \rangle, \sigma} \left(c_{i\sigma}^\dagger c_{j\sigma} + \mathrm{H.c.} \right)$$
$$+ V \sum_i \left(n_{i\uparrow} - \tfrac{1}{2} \right)\left(n_{i\downarrow} - \tfrac{1}{2} \right). \tag{2}$$

Here $c_{i\sigma}^\dagger$ and $c_{i\sigma}$ are fermionic creation and annihilation operators on site i, with $\sigma = \uparrow, \downarrow$ being the spin index. In the spinless t-V model the spin index is omitted. Fermionic operators satisfy the usual anticommutation relations, $\{c_{i\sigma}, c_{j\tau}^\dagger\} = \delta_{ij}\,\delta_{\sigma\tau}$. The parameters t_{hop} and V refer to the hopping amplitude and interaction strength, respectively. We set $t_{\mathrm{hop}} = 1$ unless stated otherwise. The symbol $\langle i,j \rangle$ labels pairs of nearest–neighbour sites. We adopt the convention $\hbar = 1$ and $k_{\mathrm{B}} = 1$ throughout the paper. In one dimension both models are integrable [66, 67].

We choose the total current along a fixed lattice direction, $\hat{x}$, as an observable of interest. For the Hubbard model the current reads

$$J = -i \sum_{i,\sigma} \left(c_{i\sigma}^\dagger c_{i+\hat{x},\sigma} - c_{i+\hat{x},\sigma}^\dagger c_{i\sigma} \right), \tag{3}$$

where $i + \hat{x}$ denotes the nearest neighbour of site i displaced by one lattice spacing along the chosen direction (in one dimension this reduces to $i+1$). For the t-V model the current is given by the same formula with subscripts σ dropped.

Autocorrelation function and moments. We introduce an inner product in the space of operators according to $(A|B) \equiv \mathrm{tr}(A^\dagger B)/\dim(\mathcal{H})$, where A and B are arbitrary operators and $\dim(\mathcal{H})$ is the (finite) Hilbert space dimension. The corresponding operator norm reads $\|A\| = \sqrt{(A|A)}$.

We wish to compute the dynamical infinite-temperature autocorrelation function of the current defined as

$$C(t) \equiv \frac{(J(t)|J)}{\|J\|^2}. \tag{4}$$

Here $J(t) = e^{it\mathcal{L}}J$ is the current operator (3) in the Heisenberg representation, with $\mathcal{L} \equiv [H, \cdot]$ being the Liouvillian superoperator acting on the space of operators.

Note that since the models we consider conserve the total number of fermions (in the Hubbard model – separately for each polarization), the equilibrium state of the system is characterized by average density of fermions, in addition to temperature. The above definition of the autocorrelation function corresponds to half-filling, i.e. to $\langle n_j \rangle = 1/2$ and $\langle n_{j\sigma} \rangle = 1/2$ for the t-V and Hubbard models, respectively.

Moments of the autocorrelation function are defined as

$$\mu_{2n} \equiv \frac{(\mathcal{L}^{2n}J|J)}{\|J\|^2} = \frac{(\mathcal{L}^n J|\mathcal{L}^n J)}{\|J\|^2} = (-1)^n \frac{d^{2n}}{dt^{2n}}C(t)\big|_{t=0}. \tag{5}$$

Note that this definition implies $\mu_0 = 1$.

Importantly, moments are polynomials of Hamiltonian parameters. Specifically, for the Hamiltonians (1) and (2), the moments (5) are polynomials in V, $\mu_{2n}(V) = \sum_{k=1}^n c_k^{(n)} V^{2k}$. In addition, the fermionic commutation relations ensure that coefficients $c_k^{(n)}$ for the current operator (3) are rational numbers. In case of $t_{\mathrm{hop}} \neq 1$, the moments scale as $\mu_{2n}(t_{\mathrm{hop}}, V) = (t_{\mathrm{hop}})^{2n}\mu_{2n}(V/t_{\mathrm{hop}})$.

The core routine of our code outputs the first $n_{\max}$ moments as polynomials in the system parameters. The computation is performed directly in the thermodynamic limit. We have obtained the sets of coefficients $c_k^{(n)}$ [68] for the Hamiltonians (1) and (2) in one, two and three dimensions. For example, the first few moments of the one-dimensional t–V model (1) read

$$2\mu_2(V) = V^2,$$
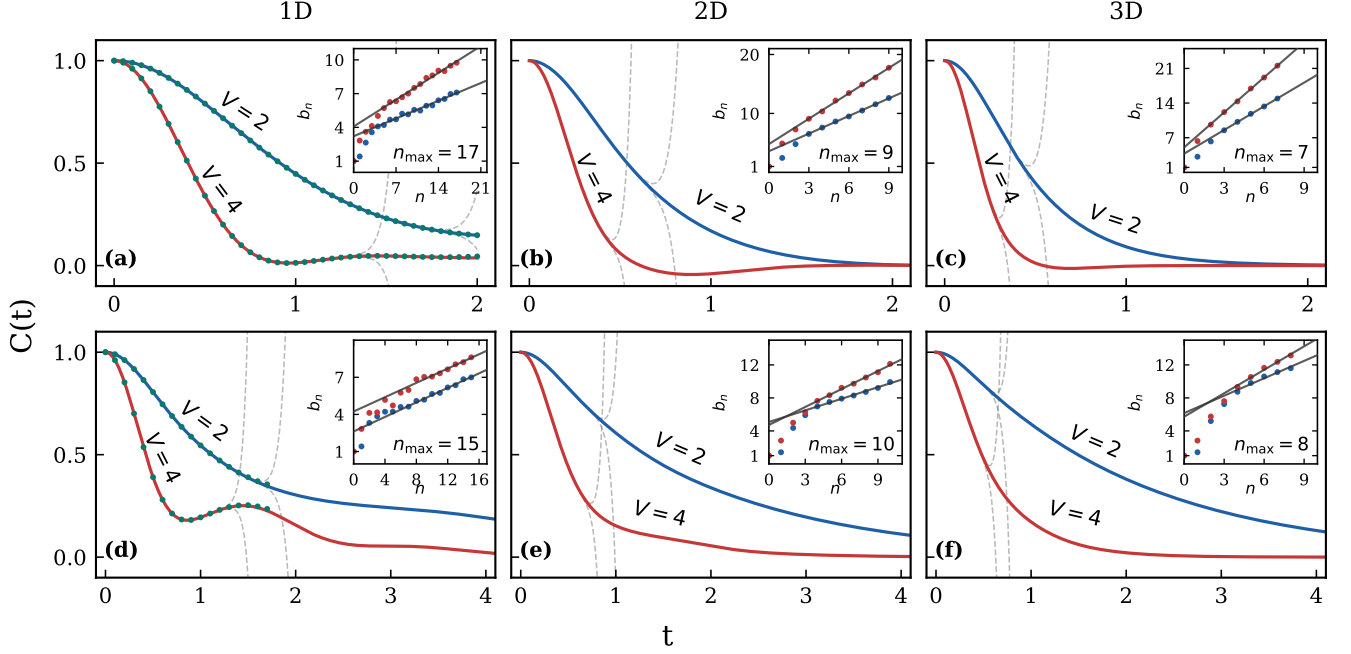$$2\mu_4(V) = 5V^2 + V^4,$$
$$2\mu_6(V) = 70V^2 + 21V^4 + V^6. \tag{6}$$

FIG. 2. Dynamical infinite-temperature autocorrelation function (4). Top row: spinless-fermion t-V model (1). Bottom row: Hubbard model (2). Solid lines: results of the recursion method in the thermodynamic limit for the two values of interaction strengths V. Gray dashed lines indicate upper and lower Taylor polynomial bounds (7). Green dots in panels (a) and (d) display the exact diagonalization results for finite periodic chains (of lengths 12 and 7, respectively) evaluated for times small enough to be representative for the thermodynamic limit. Insets show the Lanczos coefficients and their linear extrapolation.

Once the first $n_{\max}$ moments are computed, one can extract rich information about $C(t)$. In particular, one can obtain upper and lower bounds on the autocorrelation function [69–72]. The simplest bound reads [52]

$$P_{4l\pm2}(t) \leq C(t) \leq P_{4l}(t), \tag{7}$$

where $P_m(t)$ are Taylor polynomials of order m constructed from the moments of order m or less [65]. The bounds (7) are extremely tight initially but rapidly diverge at later times. The scope of these bounds is ultimately limited by the convergence radius t^* of the Taylor expansion, which is finite for 2D and 3D systems [41].

Although not the central result of the present work, the above bounds serve as a valuable benchmark for the early-time dynamics of $C(t)$, in some cases extending to relatively long times. We provide the moments required to construct these bounds in symbolic form [68], making them readily available for straightforward benchmarking of other numerical methods and quantum simulations of the t-V and Hubbard models for arbitrary values of interaction strength.

Lanczos coefficients and UOGH. The first and most important step of the recursion method is constructing an orthonormal Lanczos basis $\{O^0, O^1, O^2, \dots\}$ in which the Liouvillian $\mathcal{L}$ is tridiagonal. This basis is constructed recursively as follows: $O^0 = J/\|J\|$, $A^1 = \mathcal{L}O^0$, $b_1 = \|A^1\|$, $O^1 = b_1^{-1} A^1$ and $A^n = \mathcal{L}O^{n-1} - b_{n-1}O^{n-2}$,

$b_n = \|A^n\|$, $O^n = b_n^{-1}A^n$ for $n \geq 2$, with A^n being unnormalized counterparts of O^n. The coefficients b_n are referred to as *Lanczos coefficients*. One can straightforwardly check that $\mathcal{L}$ is indeed tridiagonal in this basis: $(O^m|\mathcal{L}O^n) = \delta_{m\,n-1}b_n + \delta_{m\,n+1}b_m$.

In fact, Lanczos coefficients b_n can be obtained directly from moments μ_{2n} [35]. We employ this relation reviewed in [65] to symbolically compute Lanczos coefficients as functions of the interaction strength for the t-V and Hubbard models in one, two and three dimensions, with the results illustrated in Fig 2.

An important question is the asymptotic behavior of Lanczos coefficients at large n. It can be proven for locally interacting systems that b_n can not grow with n faster than linear (with an additional logarithmic correction for one-dimensional systems) [41]. The UOGH [41] asserts that for chaotic quantum many-body systems this bound is saturated, i.e

$$b_n = \alpha n + \gamma + o(1) \qquad \text{as} \qquad n \to \infty \tag{8}$$

in two and three spatial dimensions. For integrable systems the scaling is not universal: while typically it is either $\sqrt{n}$ or $O(1)$ [41], linear scaling has also been observed [73–78].

The UOGH has been previously probed in various spin-1/2 systems on one- [41, 43, 79, 80], two- [43, 52, 80] and three-dimensional [55] lattices, for higher-spin systems

on one- and two-dimensional lattices [56], as well as for a three-site system of interacting bosons [81]. A rigorous proof of the UOGH has been obtained for a class of spin-1/2 systems on hypercubic lattices [82]. Finally, the UOGH has been confirmed [41] for the exactly solvable Sachdev–Ye–Kitaev model [83, 84] that describes fermions with random infinite-range couplings.

Here we probe the UOGH for locally interacting nonintegrable fermionic systems in two and three dimensions. Our results are clearly consistent with the linear asymptotic scaling of b_n for the 2D and 3D t-V model, see the insets in Fig. 2 (b), (c), as well as for the 2D Hubbard model, see the inset in Fig. 2 (e).

For the 3D Hubbard model, the linear asymptotics of the Lanczos coefficients is not apparent from our data shown in Fig. 2(f), likely due to the limited number of coefficients we can compute. We therefore treat the asymptotic linear growth of b_n in this model as a working assumption, which we adopt for the subsequent analysis.

Remarkably, we also observe the approximately linear scaling for the one-dimensional t-V and Hubbard models, which is somewhat unexpected for Bethe-ansatz-integrable models. We leave the discussion of the origin and implications of this fact for further work.

Applying the recursion method. The recursion method strengthened by the UOGH has proved highly useful in accessing dynamics at times beyond t^* [41, 44, 52, 55]. The method as such is nothing else but solving coupled Heisenberg equations in the Lanczos basis. When specified for finding the autocorrelation function, the method amounts to solving coupled differential equations,

$$\partial_t \varphi_n(t) = -b_{n+1}\varphi_{n+1}(t) + b_n\varphi_{n-1}(t), \qquad n = 0, 1, 2, \ldots \tag{9}$$

with the convention $\varphi_{-1}(t) = 0$ and initial condition $\varphi_n(0) = \delta_{n0}$. The autocorrelation function is then found from $C(t) = \varphi_0(t)$.

However, the number $n_{\max}$ of Lanczos coefficients that can be explicitly computed is necessarily limited, since the size of nested commutators $[H, J]^{(n)}$ grows exponentially with n. If we were to truncate the infinite system of equations at $n = n_{\max}$, the resulting approximation would be too rough to access the long-time dynamics of $C(t)$. Fortunately, this limitation can be overcome by extrapolating the unknown Lanczos coefficients for $n > n_{\max}$ according to the UOGH (8). This approach has already proven successful for strongly-correlated spin systems [41, 44, 52, 55]. Here we apply it to fermionic systems.

Specifically, we employ the linear fit (8) to extrapolate the Lanczos coefficients for $n > n_{\max}$, while for $n \leq n_{\max}$ the exact values of b_n are used. The resulting hybrid set of coefficients is then substituted into eq. (9). In practice, the system (9) is truncated at a finite value
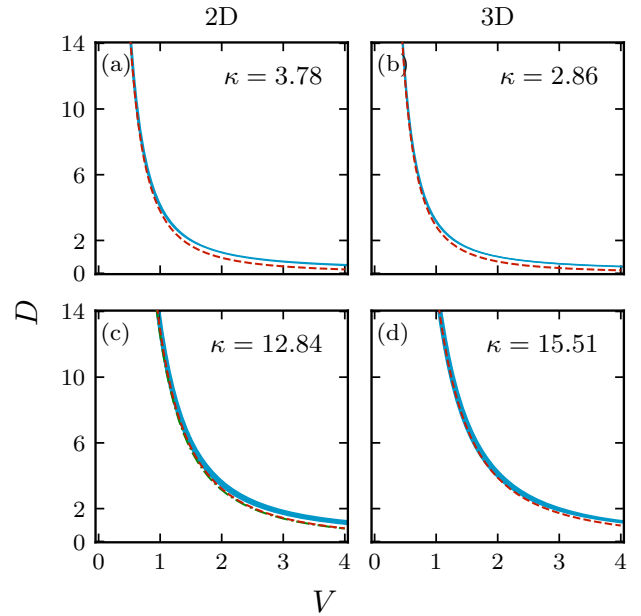

FIG. 3. Diffusion constant at half-filling in the infinite-temperature limit as a function of the interaction strength. Top row: spinless-fermion t-V model (1). Bottom row: Hubbard model (2). Solid blue – the results of the recursion method, with the width of the curve indicating the estimated uncertainty. Dashed red – the κ/V^2 fit. For the 2D Hubbard model, this fit is consistent with the perturbative result of ref[85], see [65] for details.

$K \gg n_{\max}$, chosen such that the dynamics in the chosen time window is unaffected by the truncation. For all calculations reported here we use $K = 1000$.

In Fig. 2 we show the time evolution of the current autocorrelation function (4) for the models (1) and (2) in one, two, and three spatial dimensions. Results are shown for two representative values of the interaction strength in the intermediate-to-strong coupling regime, $V = 2$ and $V = 4$. In one dimension, our results are benchmarked against exact diagonalization. In all dimensions, they are additionally benchmarked by upper and lower bounds (7). We find that the recursion method computes the autocorrelation function up to thermalization times, capturing all relevant dynamical timescales.

Transport. The knowledge of current-current autocorrelation function unlocks transport properties of the system through the Kubo linear response theory [86]. In particular, the direct-current (dc) conductivity, σ_{dc}, and the charge diffusion constant, D, read $\sigma_{\mathrm{dc}} = \beta \mathcal{V}^{-1} \mathrm{Re} \int_0^\infty dt \langle J(t)J \rangle_\beta$ and $D = \delta N_{\mathrm{tot}}^{-2} \mathrm{Re} \int_0^\infty dt \langle J(t)J \rangle_\beta$ respectively. Here $\beta = 1/T$ is the inverse temperature, $\mathcal{V}$ is the number of lattice sites, $\langle \ldots \rangle_\beta$ is the thermal average, $N_{\mathrm{tot}} = \sum_{i,\sigma} n_{i\sigma}$ is the total number of fermions and $\delta N_{\mathrm{tot}}^2 = \langle N_{\mathrm{tot}}^2 \rangle_\beta - \langle N_{\mathrm{tot}} \rangle_\beta^2$. At infinite temperature, $\langle J(t)J \rangle_\beta = \|J\|^2 C(t)$ with $C(t)$

defined by eq.(4). In fact, the integral over the current-current autocorrelation function can be effectively extracted directly from the Lanczos coefficients [87–89], which facilitates transport calculations [52, 88, 89]. In the high-temperature limit, the diffusion constant saturates at a finite value, while the dc conductivity scales linearly with the inverse temperature,

$$\sigma_{\rm dc} \simeq \beta \, \mathcal{V}^{-1} \left(\delta N_{\rm tot}^2 \, D \big|_{\beta=0} \right). \qquad (10)$$

In Fig. 3, we present the infinite-temperature diffusion constants for two- and three-dimensional t-V and Hubbard models as functions of the interaction strength V (calculations are detailed in [65]). Perturbation theory predicts $D \sim 1/V^2$ at small V [90, 91]. Surprisingly, we find that this scaling extends to quite large values of V, far beyond the expected range of applicability of the perturbation theory.

There exists a compelling experimental [92] and theoretical [90–94] evidence that the linear scaling of conductivity with β, as expressed in Eq. (10), remains valid down to relatively low temperatures on the order of 1 or even less. Combined with this observation, our calculations yield results for the dc conductivity across a wide range of interaction strengths and temperatures.

Our result for the diffusion constant in the 2D Hubbard model is consistent with a recent *tour de force* perturbative calculation reported in Ref. [85]. Notably, the latter study has culminated several earlier attempts [90, 91] that had missed certain relevant leading-order perturbative contributions. The intricacy of this perturbative calculation underscores the nontrivial nature of the hight-temperature quantum transport.

Summary and outlook We have implemented the symbolic recursion method for strongly interacting fermions on two and three dimensional lattices, focusing on t-V and Hubbard models. The method yields moments and Lanczos coefficients of dynamic autocorrelation functions as symbolic computer formulas involving model parameters. We have verified that the Lanczos coefficients for the above locally interacting fermionic models are generally consistent with the universal operator growth hypothesis (UOGH). It has been demonstrated that the recursion method supplemented by UOGH is capable of computing dynamical correlation functions up to thermalization times and accurately predicting transport properties. As an illustration, we have computed the diffusion constant in the limit of infinite temperature and the dc conductivity at temperatures above the model bandwidths. Quite unexpectedly, we have found that the diffusion constant obeys a simple scaling law over a broad range of interaction strengths.

Our work paves the way for further developments of operator-based methods in fermionic systems. Immediate extensions include reducing computational complexity by exploiting additional symmetries [95] – beyond the translational symmetry employed here – as well as applying the method to quench dynamics [47, 55] and extending it to finite temperatures [96].

Our work also demonstrates the remarkable effectiveness of a symbolic computational workflow: a single up-front computational investment yields a reusable symbolic formula that allows for subsequent efficient evaluation of dynamical and transport quantities for arbitrary model parameters. This paradigm, bridging analytic insights with computational scalability, opens new pathways for systematically exploring correlated quantum matter beyond the reach of conventional numerical methods.

END MATTER

Here, we discuss technical aspects of computing commutators in the basis of Majorana strings and the moments (5). To compute the n-fold nested commutator $[H(V), J]^{(n)}$, we employ an operator basis of Majorana strings. A Majorana string is a product of Majorana operators in the canonical order, $\Gamma = \gamma_{i_1,\sigma_1} \gamma_{i_2,\sigma_2} \cdots \gamma_{i_l,\sigma_l}$, where $\gamma_{2j-1,\sigma} = c_{j\sigma} + c_{j\sigma}^\dagger$ and $\gamma_{2j,\sigma} = -i(c_{j\sigma} - c_{j\sigma}^\dagger)$. The canonical order implies that (i) the site labels are arranged in the strictly increasing order, $i_1 < i_2 < \cdots < i_l$ and (ii) for each site, the spin-down operator is placed before the spin-up operator, i.e., $\gamma_{j,\downarrow} \gamma_{j,\uparrow}$. For a system of spinless (spinful) fermions on $\mathcal{V}$ sites, there are in total $\mathcal{D} = 4^{\mathcal{V}}$ ($\mathcal{D} = 4^{2\mathcal{V}}$) canonical Majorana strings Γ_s, which form an operator basis $\mathcal{G} = \{\Gamma_s\}_{s=1}^{\mathcal{D}}$ orthogonal with respect to the inner product introduced earlier.

Any fermionic operator can be uniquely decomposed in this basis of Majorana strings. Consequently, the n-fold commutator can be written as

$$[H(V), J]^{(n)} = \sum_{k=1}^{\mathcal{N}_n} a_k \Gamma_k, \qquad (11)$$

where a_k are complex coefficients and $\mathcal{N}_n$ denotes the number of nonzero Majorana strings appearing at order n.

In computer memory, each Majorana string Γ_k is stored as an ordered list of indices, while the coefficients a_k may be represented using finite-precision arithmetic, infinite-precision arithmetic, or in symbolic form. Our numerical routines operate directly in the space of Majorana strings. In practice, we first express the Hamiltonians (1,2) and the observable (3) in the Majorana basis, and then iteratively construct the commutators $[H, J]^{(n)}$
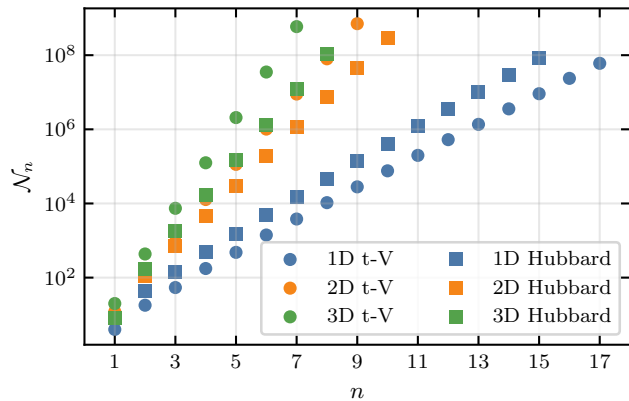
FIG. 4. Number of terms $\mathcal{N}_n$ in the n-th nested commutator (11) as a function of the commutator order n for the t–V and Hubbard models in one, two, and three dimensions.

until memory constraints are reached. Note that managing Majorana strings for fermions is strongly analogous to managing Pauli strings for qubits but requires the additional step of maintaining the canonical operator ordering, which incurs extra computational overhead. This extra step increases computational time as each string must be ordered, but does not increase the memory required.

Using infinite-precision arithmetic, the largest operators we obtained for the two-dimensional t–V model (1) at $k = 9$ contain $\mathcal{N}_9^{\text{2D-tV}} \simeq 7 \times 10^8$ Majorana strings and occupy approximately 43 GB of memory, corresponding to an average of ~ 60 bytes per string. The number of terms $\mathcal{N}_n$ grows exponentially with n, see Fig. 4. For example, in the three-dimensional Hubbard model we observe $\mathcal{N}_n^{\text{3D-Hub}} \sim 10^n$, making each subsequent moment roughly an order of magnitude more expensive to compute than the previous one.

Although our framework allows us to keep the coefficients a_k in symbolic form and thereby construct *symbolic surrogates* [58, 97] of the operators $[H(V), J]^{(n)}$, this is not required to obtain symbolic expressions for the moments $\mu_{2n}(V)$. Since $\mu_{2n}(V)$ is a polynomial in V of degree $2n$, it is sufficient to compute the moments at $2n + 1$ distinct values of V using infinite-precision arithmetic and then reconstruct the full polynomial via interpolation. This strategy trades computational time for memory and enables access to higher-order moments in memory-limited settings.

Symbolic Majorana strings are also utilized in a recently proposed Majorana propagation method [27]. This method mostly focuses on simulating fermionic quantum circuits, but can also be applied to simulations of real-time dynamics by approximating the actual Heisenberg evolution by discrete Trotter steps. Recent applications of the method to small finite two-dimensional Hubbard models show that Majorana propagation is efficient in

the case of small interaction strength V [28], but can face limitations for larger values of V [28, 33].

---

* ermakov1054@yandex.ru
† lychkovskiy@gmail.com

[1] Robert B Laughlin. Anomalous quantum Hall effect: An incompressible quantum fluid with fractionally charged excitations. *Physical Review Letters*, 50(18):1395, 1983.

[2] Elbio Dagotto. Correlated electrons in high-temperature superconductors. *Reviews of Modern Physics*, 66(3):763, 1994.

[3] Masatoshi Imada, Atsushi Fujimori, and Yoshinori Tokura. Metal-insulator transitions. *Reviews of modern physics*, 70(4):1039, 1998.

[4] Yoshinori Tokura. Correlated-electron physics in transition-metal oxides. *Physics Today*, 56(7):50–55, 2003.

[5] Matthias Troyer and Uwe-Jens Wiese. Computational complexity and fundamental limitations to fermionic quantum Monte Carlo simulations. *Physical review letters*, 94(17):170201, 2005.

[6] Peter T Brown, Debayan Mitra, Elmer Guardado-Sanchez, Reza Nourafkan, Alexis Reymbaut, Charles-David Hébert, Simon Bergeron, A-MS Tremblay, Jure Kokalj, David A Huse, et al. Bad metallic transport in a cold atom fermi-hubbard system. *Science*, 363(6425):379–382, 2019.

[7] Matthew A Nichols, Lawrence W Cheuk, Melih Okan, Thomas R Hartke, Enrique Mendez, T Senthil, Ehsan Khatami, Hao Zhang, and Martin W Zwierlein. Spin transport in a Mott insulator of ultracold fermions. *Science*, 363(6425):383–387, 2019.

[8] Elmer Guardado-Sanchez, Alan Morningstar, Benjamin M Spar, Peter T Brown, David A Huse, and Waseem S Bakr. Subdiffusion and heat transport in a tilted two-dimensional Fermi-Hubbard system. *Physical Review X*, 10(1):011042, 2020.

[9] Jeremija Kovačević, Michel Ferrero, and Jakša Vučičević. Toward numerically exact computation of conductivity in the thermodynamic limit of interacting lattice models. *Physical Review Letters*, 135(1):016502, 2025.

[10] Susumu Yamada, Toshiyuki Imamura, and Masahiko Machida. 16.447 tflops and 159-billion-dimensional exact-diagonalization for trapped Fermion-Hubbard model on the Earth simulator. In *SC'05: Proceedings of the 2005 ACM/IEEE Conference on Supercomputing*, pages 44–44. IEEE, 2005.

[11] Michael Innerberger, Paul Worm, Paul Prauhart, and Anna Kauch. Electron-light interaction in nonequilibrium: exact diagonalization for time-dependent Hubbard hamiltonians. *The European Physical Journal Plus*, 135(11):922, 2020.

[12] Tomaž Prosen. Exact nonequilibrium steady state of a strongly driven open xxz chain. *Physical review letters*, 107(13):137201, 2011.

[13] Bruno Bertini, Fabian Heidrich-Meisner, Christoph Karrasch, Tomaž Prosen, Robin Steinigeweg, and Marco Žnidarič. Finite-temperature transport in one-dimensional quantum lattice models. *Reviews of Modern Physics*, 93(2):025003, 2021.

[14] M L Wall and Lincoln D Carr. Out-of-equilibrium dynamics with matrix product states. *New Journal of Physics*, 14(12):125015, dec 2012.

[15] Thomas Barthel, Carlos Pineda, and Jens Eisert. Contraction of fermionic operator circuits and the simulation of strongly correlated fermions. *Physical Review A—Atomic, Molecular, and Optical Physics*, 80(4):042333, 2009.

[16] Christina V Kraus, Norbert Schuch, Frank Verstraete, and J Ignacio Cirac. Fermionic projected entangled pair states. *Physical Review A—Atomic, Molecular, and Optical Physics*, 81(5):052338, 2010.

[17] Philippe Corboz, Glen Evenbly, Frank Verstraete, and Guifré Vidal. Simulation of interacting fermions with entanglement renormalization. *Physical Review A—Atomic, Molecular, and Optical Physics*, 81(1):010303, 2010.

[18] Iztok Pižorn and Frank Verstraete. Fermionic implementation of projected entangled pair states algorithm. *Physical Review B—Condensed Matter and Materials Physics*, 81(24):245110, 2010.

[19] Dominic Bergeron, Vasyl Hankevych, Bumsoo Kyung, and A-MS Tremblay. Optical and dc conductivity of the two-dimensional hubbard model in the pseudogap regime and across the antiferromagnetic quantum critical point including vertex corrections. *Physical Review B—Condensed Matter and Materials Physics*, 84(8):085128, 2011.

[20] Alexey M Shakirov, Sergey V Tsibulsky, Andrey E Antipov, Yulia E Shchadilova, and Alexey N Rubtsov. Modeling the metastable dynamics of correlated structures. *Scientific Reports*, 5(1):8005, 2015.

[21] Edward Perepelitsky, Andrew Galatas, Jernej Mravlje, Rok Žitko, Ehsan Khatami, B Sriram Shastry, and Antoine Georges. Transport and optical conductivity in the hubbard model: A high-temperature expansion perspective. *Physical Review B*, 94(23):235115, 2016.

[22] Jaksa Vucicevic, Jure Kokalj, Rok Zitko, Nils Wentzell, Darko Tanaskovic, and Jernej Mravlje. Conductivity in the square lattice hubbard model at high temperatures: Importance of vertex corrections. *arXiv preprint arXiv:1811.08343*, 2018.

[23] Thomas G Kiely and Erich J Mueller. Transport in the two-dimensional fermi-hubbard model: Lessons from weak coupling. *Physical Review B*, 104(16):165143, 2021.

[24] Martin Ulaga, Jernej Mravlje, Peter Prelovšek, and Jure Kokalj. Thermal conductivity and heat diffusion in the two-dimensional hubbard model. *Physical Review B*, 106(24):245123, 2022.

[25] Martin Ulaga, Jernej Mravlje, and Jure Kokalj. Thermoelectric effect on diffusion in the two-dimensional hubbard model. *Physical Review B*, 108(15):155118, 2023.

[26] J Vučičević, S Predin, and Michel Ferrero. Charge fluctuations, hydrodynamics, and transport in the square-lattice hubbard model. *Physical Review B*, 107(15):155140, 2023.

[27] Aaron Miller, Zoë Holmes, Özlem Salehi, Rahul Chakraborty, Anton Nykänen, Zoltán Zimborás, Adam Glos, and Guillermo García-Pérez. Simulation of fermionic circuits using majorana propagation. *arXiv preprint arXiv:2503.18939*, 2025.

[28] Giorgio Facelli, Hamza Fawzi, and Omar Fawzi. Fast convergence of majorana propagation for weakly interacting fermions. *arXiv preprint arXiv:2601.05226*, 2026.

[29] Michael Schreiber, Sean S Hodgman, Pranjal Bordia, Henrik P Lüschen, Mark H Fischer, Ronen Vosk, Ehud Altman, Ulrich Schneider, and Immanuel Bloch. Observation of many-body localization of interacting fermions in a quasirandom optical lattice. *Science*, 349(6250):842–845, 2015.

[30] Frank Arute, Kunal Arya, Ryan Babbush, Dave Bacon, Joseph C Bardin, Rami Barends, Andreas Bengtsson, Sergio Boixo, Michael Broughton, Bob B Buckley, et al. Observation of separated dynamics of charge and spin in the fermi-hubbard model (2020). *arXiv preprint arXiv:2010.07965*, 7, 2010.

[31] Lucia Vilchez-Estevez, Raul A Santos, Sabrina Yue Wang, and Filippo Maria Gambetta. Extracting the spin excitation spectrum of a fermionic system using a quantum processor. *Physical Review B*, 112(4):045143, 2025.

[32] Talal Ahmed Chowdhury, Vladimir Korepin, Vincent R Pascuzzi, and Kwangmin Yu. Quantum utility in simulating the real-time dynamics of the fermi-hubbard model using superconducting quantum computers. *arXiv preprint arXiv:2509.14196*, 2025.

[33] Faisal Alam, Jan Lukas Bosse, Ieva Čepaitė, Adrian Chapman, Laura Clinton, Marcos Crichigno, Elizabeth Crosson, Toby Cubitt, Charles Derby, Oliver Dowinton, et al. Fermionic dynamics on a trapped-ion quantum computer beyond exact classical simulation. *arXiv preprint arXiv:2510.26300*, 2025.

[34] Hazime Mori. A continued-fraction representation of the time-correlation functions. *Progress of Theoretical Physics*, 34(3):399–416, 1965.

[35] Marc Dupuis. Moment and continued fraction expansions of time autocorrelation functions. *Progress of Theoretical Physics*, 37(3):502–537, 1967.

[36] Roger Haydock. The recursive solution of the schrodinger equation. In *Solid state physics*, volume 35, pages 215–294. Elsevier, 1980.

[37] Daniel C Mattis. How to reduce practically any problem to one dimension. In *Physics in One Dimension: Proceedings of an International Conference Fribourg, Switzerland, August 25–29, 1980*, pages 3–10. Springer, 1981.

[38] VS Viswanath and Gerhard Müller. *The recursion method: application to many-body dynamics*. Springer, 1994.

[39] Tarek A. Elsayed, Benjamin Hess, and Boris V. Fine. Signatures of chaos in time series generated by many-spin systems at high temperatures. *Phys. Rev. E*, 90:022910, Aug 2014.

[40] Gabriel Bouch. Complex-time singularity and locality estimates for quantum lattice systems. *Journal of Mathematical Physics*, 56(12), 2015.

[41] Daniel E Parker, Xiangyu Cao, Alexander Avdoshkin, Thomas Scaffidi, and Ehud Altman. A universal operator growth hypothesis. *Physical Review X*, 9(4):041017, 2019.

[42] Alexander Avdoshkin and Anatoly Dymarsky. Euclidean operator growth and quantum chaos. *Phys. Rev. Res.*, 2:043234, Nov 2020.

[43] Ayush De, Umberto Borla, Xiangyu Cao, and Snir Gazit. Stochastic sampling of operator growth dynamics. *Phys. Rev. B*, 110:155135, Oct 2024.

[44] Alexander Teretenkov, Filipp Uskov, and Oleg Lychkovskiy. Pseudomode expansion of many-body correlation functions. *Phys. Rev. B*, 111:174308, May 2025.

[45] Pratik Nandy, Apollonas S Matsoukas-Roubeas, Pablo

Martínez-Azcona, Anatoly Dymarsky, and Adolfo del Campo. Quantum dynamics in krylov space: Methods and applications. *Physics Reports*, 1125:1–82, 2025.

[46] Oleksandr Gamayun, Murtaza Ali Mir, Oleg Lychkovskiy, and Zoran Ristivojevic. Exactly solvable models for universal operator growth. *J. High Energ. Phys.*, 2025:256, 2025.

[47] Nicolas Loizeau, Berislav Buča, and Dries Sels. Opening krylov space to access all-time dynamics via dynamical symmetries. *Physical Review Letters*, 135(20):200401, 2025.

[48] Gabriele Pinna, Oliver Lunt, and Curt von Keyserlingk. Approximation theory for green's functions via the lanczos algorithm. *Phys. Rev. B*, 112:054435, Aug 2025.

[49] VS Viswanath, Shu Zhang, Joachim Stolze, and Gerhard Müller. Ordering and fluctuations in the ground state of the one-dimensional and two-dimensional s= 1/2 xxz antiferromagnets: A study of dynamical properties based on the recursion method. *Physical Review B*, 49(14):9702, 1994.

[50] Daniel J Yates, Alexander G Abanov, and Aditi Mitra. Lifetime of almost strong edge-mode operators in one-dimensional, interacting, symmetry protected topological phases. *Physical Review Letters*, 124(20):206803, 2020.

[51] Daniel J Yates, Alexander G Abanov, and Aditi Mitra. Dynamics of almost strong edge modes in spin chains away from integrability. *Physical Review B*, 102(19):195419, 2020.

[52] Filipp Uskov and Oleg Lychkovskiy. Quantum dynamics in one and two dimensions via the recursion method. *Phys. Rev. B*, 109:L140301, Apr 2024.

[53] Nicolas Loizeau, J. Clayton Peacock, and Dries Sels. Quantum many-body simulations with PauliStrings.jl. *SciPost Phys. Codebases*, page 54, 2025.

[54] Nicolas Loizeau, J. Clayton Peacock, and Dries Sels. Codebase release 1.5 for PauliStrings.jl. *SciPost Phys. Codebases*, pages 54–r1.5, 2025.

[55] Ilya Shirokov, Viacheslav Khrushchev, Filipp Uskov, Ivan Dudinets, Igor Ermakov, and Oleg Lychkovskiy. Quench dynamics via recursion method and dynamical quantum phase transitions. *arXiv preprint arXiv:2503.24362*, 2025.

[56] Igor Ermakov. Operator growth in many-body systems of higher spins. *arXiv preprint arXiv:2504.07833*, 2025.

[57] Tibor Rakovszky, C. W. von Keyserlingk, and Frank Pollmann. Dissipation-assisted operator evolution method for capturing hydrodynamic transport. *Phys. Rev. B*, 105:075131, Feb 2022.

[58] Manuel S Rudolph, Enrico Fontana, Zoë Holmes, and Lukasz Cincio. Classical surrogate simulation of quantum systems with LOWESA. *arXiv preprint arXiv:2308.09109*, 2023.

[59] Igor Ermakov, Oleg Lychkovskiy, and Tim Byrnes. Unified framework for efficiently computable quantum circuits. *arXiv preprint arXiv:2401.08187*, 2024.

[60] Thomas Schuster, Chao Yin, Xun Gao, and Norman Y Yao. A polynomial-time classical algorithm for noisy quantum circuits. *Physical Review X*, 15(4):041018, 2025.

[61] Tomislav Begušić and Garnet Kin-Lic Chan. Real-time operator evolution in two and three dimensions via sparse pauli dynamics. *PRX Quantum*, 6:020302, Apr 2025.

[62] Armando Angrisani, Antonio A Mele, Manuel S Rudolph, M Cerezo, and Zoe Holmes. Simulating quantum circuits with arbitrary local noise using pauli propagation. *arXiv preprint arXiv:2501.13101*, 2025.

[63] Manuel S Rudolph, Tyson Jones, Yanting Teng, Armando Angrisani, and Zoë Holmes. Pauli propagation: A computational framework for simulating quantum systems. *arXiv preprint arXiv:2505.21606*, 2025.

[64] Stuart Yi-Thomas, Brayden Ware, Jay D. Sau, and Christopher David White. Comparing numerical methods for hydrodynamics in a one-dimensional lattice spin model. *Phys. Rev. B*, 110:134308, Oct 2024.

[65] See Supplementary Material for the details on Majorana strings and Hamiltonians in terms of Majorana Fermions, transport calculations and the relation between moments and Lanczos coefficients.

[66] Elliott H. Lieb and F. Y. Wu. Absence of mott transition in an exact solution of the short-range, one-band model in one dimension. *Phys. Rev. Lett.*, 20:1445–1448, Jun 1968.

[67] Minoru Takahashi. *Thermodynamics of one-dimensional solvable models*. Cambridge university press, Cambridge, 1999.

[68] Symbolic expressions for moments are avaliable at the repository. https://github.com/ns1gn/symbolic-moments-tV-Hubbard.

[69] Ole Platz and Roy G. Gordon. Rigorous bounds for time-dependent correlation functions. *Phys. Rev. Lett.*, 30:264–267, Feb 1973.

[70] JoséM.R. Roldan, Barry M. McCoy, and Jacques H.H. Perk. Dynamic spin correlation functions of the xyz chain at infinite temperature: A study based on moments. *Physica A: Statistical Mechanics and its Applications*, 136(2):255–302, 1986.

[71] Uwe Brandt and Joachim Stolze. High-temperature dynamics of the anisotropic heisenberg chain studied by moment methods. *Zeitschrift für Physik B Condensed Matter*, 64(3):327–339, 1986.

[72] M Bohm and H Leschke. Dynamic spin-pair correlations in a heisenberg chain at infinite temperature based on an extended short-time expansion. *Journal of Physics A: Mathematical and General*, 25(5):1043, mar 1992.

[73] Anatoly Dymarsky and Michael Smolkin. Krylov complexity in conformal field theory. *Phys. Rev. D*, 104:L081702, Oct 2021.

[74] Budhaditya Bhattacharjee, Xiangyu Cao, Pratik Nandy, and Tanay Pathak. Krylov complexity in saddle-dominated scrambling. *Journal of High Energy Physics*, 2022(5):1–27, 2022.

[75] Hugo A Camargo, Viktor Jahnke, Keun-Young Kim, and Mitsuhiro Nishida. Krylov complexity in free and interacting scalar field theories with bounded power spectrum. *Journal of High Energy Physics*, 2023(5):1–48, 2023.

[76] Alexander Avdoshkin, Anatoly Dymarsky, and Michael Smolkin. Krylov complexity in quantum field theory, and beyond. *Journal of High Energy Physics*, 2024(6):1–29, 2024.

[77] MJ Vasli, K Babaei Velni, MR Mohammadi Mozaffar, A Mollabashi, and M Alishahiha. Krylov complexity in lifshitz-type scalar field theories. *The European Physical Journal C*, 84(3):235, 2024.

[78] Peng-Zhang He and Hai-Qing Zhang. Krylov complexity in the schrödinger field theory. *Journal of High Energy Physics*, 2025(3):1–35, 2025.

[79] Jae Dong Noh. Operator growth in the transverse-field ising spin chain with integrability-breaking longitudinal field. *Phys. Rev. E*, 104:034112, Sep 2021.

[80] Robin Heveling, Jiaozi Wang, and Jochen Gemmer. Numerically probing the universal operator growth hypothesis. *Phys. Rev. E*, 106:014152, Jul 2022.

[81] Arpan Bhattacharyya, Debodirna Ghosh, and Poulami Nandi. Operator growth and krylov complexity in bose-hubbard model. *Journal of High Energy Physics*, 2023(12):1–25, 2023.

[82] Xiangyu Cao. A statistical mechanism for operator growth. *Journal of Physics A: Mathematical and Theoretical*, 54(14):144001, mar 2021.

[83] Subir Sachdev and Jinwu Ye. Gapless spin-fluid ground state in a random quantum heisenberg magnet. *Physical Review Letters*, 70(21):3339–3342, 1993.

[84] Juan Maldacena and Douglas Stanford. Remarks on the sachdev–ye–kitaev model. *Physical Review D*, 94(10):106002, 2016.

[85] Jeremija Kovačević, Michel Ferrero, and Jak ša Vučičević. Toward numerically exact computation of conductivity in the thermodynamic limit of interacting lattice models. *Phys. Rev. Lett.*, 135:016502, Jul 2025.

[86] Gerald D Mahan. *Many-particle physics*. Springer Science & Business Media, 2013.

[87] C.G. Joslin and C.G. Gray. Calculation of transport coefficients using a modified mori formalism. *Molecular Physics*, 58(4):789–797, 1986.

[88] Jiaozi Wang, Mats H. Lamann, Robin Steinigeweg, and Jochen Gemmer. Diffusion constants from the recursion method. *Phys. Rev. B*, 110:104413, Sep 2024.

[89] Christian Bartsch, Anatoly Dymarsky, Mats H. Lamann, Jiaozi Wang, Robin Steinigeweg, and Jochen Gemmer. Estimation of equilibration time scales from nested fraction approximations. *Phys. Rev. E*, 110:024126, Aug 2024.

[90] Thomas G. Kiely and Erich J. Mueller. Transport in the two-dimensional fermi-hubbard model: Lessons from weak coupling. *Phys. Rev. B*, 104:165143, Oct 2021.

[91] J. Vučičević, S. Predin, and M. Ferrero. Charge fluctuations, hydrodynamics, and transport in the square-lattice hubbard model. *Phys. Rev. B*, 107:155140, Apr 2023.

[92] Peter T. Brown, Debayan Mitra, Elmer Guardado-Sanchez, Reza Nourafkan, Alexis Reymbaut, Charles-David Hébert, Simon Bergeron, A.-M. S. Tremblay, Jure Kokalj, David A. Huse, Peter Schauß, and Waseem S. Bakr. Bad metallic transport in a cold atom Fermi-Hubbard system. *Science*, 363(6425):379–382, 2019.

[93] Connie H. Mousatov, Ilya Esterlis, and Sean A. Hartnoll. Bad metallic transport in a modified hubbard model. *Phys. Rev. Lett.*, 122:186601, May 2019.

[94] A. Vranić, J. Vučičević, J. Kokalj, J. Skolimowski, R. Žitko, J. Mravlje, and D. Tanasković. Charge transport in the hubbard model at high temperatures: Triangular versus square lattice. *Phys. Rev. B*, 102:115142, Sep 2020.

[95] Yanting Teng, Su Yeon Chang, Manuel S Rudolph, and Zoë Holmes. Leveraging symmetry merging in pauli propagation. *arXiv preprint arXiv:2512.12094*, 2025.

[96] Nikolaos Angelinos, Debarghya Chakraborty, and Anatoly Dymarsky. Temperature dependence in krylov space. *arXiv preprint arXiv:2508.19233*, 2025.

[97] Enrico Fontana, Manuel S Rudolph, Ross Duncan, Ivan Rungger, and Cristina Cîrstoiu. Classical simulations of noisy variational quantum circuits. *npj Quantum Information*, 11(1):84, 2025.

Supplementary Material for:
"Symbolic recursion method for strongly correlated fermions in two and three dimensions"

Igor Ermakov[1, 2, 3, *] and Oleg Lychkovskiy[4, 3, †]

[1] *Wilczek Quantum Center, Shanghai Institute for Advanced Studies,*
University of Science and Technology of China, Shanghai 201315, China
[2] *Hefei National Laboratory, Hefei 230088, China*
[3] *Department of Mathematical Methods for Quantum Technologies,*
Steklov Mathematical Institute of Russian Academy of Sciences, 8 Gubkina St., Moscow 119991, Russia.
[4] *Skolkovo Institute of Science and Technology, Bolshoy Boulevard 30, bld. 1, Moscow 121205, Russia.*

(Dated: January 27, 2026)

CONTENTS

OPERATOR BASIS OF MAJORANA STRINGS

Fermionic operators and Majorana fermions

We consider a lattice system of fermions with sites labeled by $j = 1, \ldots, L$. Each site might carry an additional spin index $\sigma \in \{\uparrow, \downarrow\}$. For spinless fermions the spin index is omitted in all the below formulas.

Let us start with the definition of the fermionic annihilation and creation operators $c_{j\sigma}$ and $c_{j\sigma}^\dagger$. These operators satisfy the canonical anticommutation relations

$$\{c_{i\sigma}, c_{j\tau}^\dagger\} = \delta_{ij}\,\delta_{\sigma\tau}, \qquad \{c_{i\sigma}, c_{j\tau}\} = 0, \qquad \{c_{i\sigma}^\dagger, c_{j\tau}^\dagger\} = 0. \tag{S1}$$

We introduce Majorana fermions by doubling the lattice index for each fermionic mode as:

$$\gamma_{2j-1,\sigma} = c_{j\sigma} + c_{j\sigma}^\dagger, \qquad \gamma_{2j,\sigma} = -i\,(c_{j\sigma} - c_{j\sigma}^\dagger). \tag{S2}$$

These operators are Hermitian, $\gamma_{k,\sigma}^\dagger = \gamma_{k,\sigma}$, and satisfy $\gamma_{k,\sigma}^2 = 1$. The inverse transformation reads:

$$c_{j\sigma} = \tfrac{1}{2}(\gamma_{2j-1,\sigma} + i\,\gamma_{2j,\sigma}), \qquad c_{j\sigma}^\dagger = \tfrac{1}{2}(\gamma_{2j-1,\sigma} - i\,\gamma_{2j,\sigma}). \tag{S3}$$

In the spinless case one simply drops the spin index σ, so that each site j is associated with two Majorana operators γ_{2j-1} and γ_{2j}.

Clifford algebra

Majorana operators obey the Clifford algebra:

$$\{\gamma_{k,\sigma}, \gamma_{\ell,\tau}\} = 2\,\delta_{k\ell}\,\delta_{\sigma\tau}. \tag{S4}$$

Their commutator can be written as

$$[\gamma_{k,\sigma}, \gamma_{\ell,\tau}] = \begin{cases} 0, & (k,\sigma) = (\ell,\tau), \\ 2\,\gamma_{k,\sigma}\gamma_{\ell,\tau}, & \text{otherwise.} \end{cases} \tag{S5}$$

Majorana strings and canonical ordering

Let us introduce an operator basis of Majorana strings. A Majorana string is defined as a product of Majorana operators:

$$\Gamma = \gamma_{i_1,\sigma_1}\gamma_{i_2,\sigma_2}\cdots\gamma_{i_\ell,\sigma_\ell}. \tag{S6}$$

We fix a canonical form of Majorana strings by imposing the following ordering rules:

1. the lattice indices are strictly increasing, $i_1 < i_2 < \cdots < i_\ell$;

2. for Majorana operators acting on the same lattice site, the spin-up operator precedes the spin-down operator, $\gamma_{j,\uparrow}\gamma_{j,\downarrow}$.

In the spinless case only the first condition applies.

Scalar product

We now introduce the inner product in the operator space employed throughout this work. At infinite temperature it is defined as

$$(A|B) \equiv \frac{\mathrm{tr}(A^\dagger B)}{\dim(\mathcal{H})}, \tag{S7}$$

where $\dim(\mathcal{H})$ denotes the (finite) dimension of the many-body Hilbert space. The corresponding operator norm is defined as

$$\|A\| = \sqrt{(A|A)}. \tag{S8}$$

With respect to this inner product, distinct canonical Majorana strings are mutually orthogonal. More precisely, for two canonical Majorana strings Γ_s and $\Gamma_{s'}$ one finds

$$(\Gamma_s|\Gamma_{s'}) = \delta_{ss'}. \tag{S9}$$

The set of all canonical Majorana strings forms an orthonormal basis in the space of operators. For a system with N fermionic modes, the total number of such strings is 4^N, and the corresponding operator basis is denoted as $\mathcal{G} = \{\Gamma_s\}_{s=1}^{4^N}$.

Product of Majorana strings

The product of two Majorana strings is again a Majorana string (up to an overall phase). Let us consider two canonical Majorana strings,

$$\Gamma = \gamma_{i_1,\sigma_1}\gamma_{i_2,\sigma_2}\cdots\gamma_{i_\ell,\sigma_\ell}, \qquad \Gamma' = \gamma_{j_1,\tau_1}\gamma_{j_2,\tau_2}\cdots\gamma_{j_m,\tau_m}. \tag{S10}$$

Their product is given by the concatenation of the two strings,

$$\Gamma\,\Gamma' = \gamma_{i_1,\sigma_1}\cdots\gamma_{i_\ell,\sigma_\ell}\gamma_{j_1,\tau_1}\cdots\gamma_{j_m,\tau_m}, \tag{S11}$$

which is, in general, not in canonical form.

The canonical form of the product is obtained by the following procedure:

1. *Concatenation.* The two strings are written as a single product of Majorana operators, preserving their internal order.

2. *Reordering.* The Majorana operators are reordered into canonical order using the anticommutation relations. Each exchange of two distinct Majorana operators produces a minus sign.

3. *Removal of pairs.* Whenever two identical Majorana operators become adjacent, they are removed using $\gamma_{k,\sigma}^2 = 1$.

After these steps, the product $\Gamma\,\Gamma'$ reduces to a single canonical Majorana string multiplied by an overall phase.
Example. Consider the product of two canonical Majorana strings with spin indices,

$$\Gamma = \gamma_{1,\downarrow}\gamma_{2,\downarrow}\gamma_{3,\uparrow}\gamma_{4,\uparrow}, \tag{S12}$$

$$\Gamma' = \gamma_{2,\uparrow}\gamma_{3,\uparrow}\gamma_{5,\downarrow}, \tag{S13}$$

both written in canonical order.
Step 1: by concatenation of the above strings we obtain Majorana string in non-canonical form

$$\Gamma\,\Gamma' = \gamma_{1,\downarrow}\gamma_{2,\downarrow}\gamma_{3,\uparrow}\gamma_{4,\uparrow}\gamma_{2,\uparrow}\gamma_{3,\uparrow}\gamma_{5,\downarrow}. \tag{S14}$$

Step 2:

$$\Gamma\,\Gamma' = \gamma_{1,\downarrow}\gamma_{2,\downarrow}\gamma_{3,\uparrow}\gamma_{4,\uparrow}\gamma_{2,\uparrow}\gamma_{3,\uparrow}\gamma_{5,\downarrow}$$
$$\xrightarrow{(-1)^3} -\gamma_{1,\downarrow}\gamma_{2,\uparrow}\gamma_{2,\downarrow}\gamma_{3,\uparrow}\gamma_{4,\uparrow}\gamma_{3,\uparrow}\gamma_{5,\downarrow}$$
$$\xrightarrow{(-1)^1} +\gamma_{1,\downarrow}\gamma_{2,\uparrow}\gamma_{2,\downarrow}\gamma_{3,\uparrow}\gamma_{3,\uparrow}\gamma_{4,\uparrow}\gamma_{5,\downarrow}. \tag{S15}$$

Step 3: Using $\gamma_{k,\sigma}^2 = 1$, we obtain

$$\Gamma\,\Gamma' = \gamma_{1,\downarrow}\gamma_{2,\uparrow}\gamma_{2,\downarrow}\gamma_{4,\uparrow}\gamma_{5,\downarrow}, \tag{S16}$$

which is a Majorana string in a canonical form.

HAMILTONIANS AND OBSERVABLES IN TERMS OF MAJORANA STRINGS

In this section we rewrite the Hamiltonians and the current operator used in the main text in the basis of Majorana strings.
For $i \neq j$ (and fixed σ) one obtains the standard identities

$$c_{i\sigma}^\dagger c_{j\sigma} + c_{j\sigma}^\dagger c_{i\sigma} = \frac{i}{2}\left(\gamma_{2i-1,\sigma}\gamma_{2j,\sigma} - \gamma_{2i,\sigma}\gamma_{2j-1,\sigma}\right), \tag{S17}$$

$$c_{i\sigma}^\dagger c_{j\sigma} - c_{j\sigma}^\dagger c_{i\sigma} = \frac{1}{2}\left(\gamma_{2i-1,\sigma}\gamma_{2j-1,\sigma} + \gamma_{2i,\sigma}\gamma_{2j,\sigma}\right), \tag{S18}$$

and for the density on a given site

$$n_{i\sigma} = c_{i\sigma}^\dagger c_{i\sigma} = \frac{1}{2}\left(1 + i\,\gamma_{2i-1,\sigma}\gamma_{2i,\sigma}\right), \qquad n_{i\sigma} - \tfrac{1}{2} = \frac{i}{2}\gamma_{2i-1,\sigma}\gamma_{2i,\sigma}. \tag{S19}$$

Spinless t–V model

The spinless t–V Hamiltonian in the main text reads

$$H_{\mathrm{tV}} = -t_{\mathrm{hop}}\sum_{\langle i,j\rangle}\left(c_i^\dagger c_j + \mathrm{H.c.}\right) + V\sum_{\langle i,j\rangle}\left(n_i - \tfrac{1}{2}\right)\left(n_j - \tfrac{1}{2}\right). \tag{S20}$$

Using Eqs. (S17) and (S19) (with the spin index dropped), we obtain the Majorana form

$$H_{\mathrm{tV}} = -\frac{i\,t_{\mathrm{hop}}}{2}\sum_{\langle i,j\rangle}\left(\gamma_{2i-1}\gamma_{2j} - \gamma_{2i}\gamma_{2j-1}\right) - \frac{V}{4}\sum_{\langle i,j\rangle}\gamma_{2i-1}\gamma_{2i}\gamma_{2j-1}\gamma_{2j}. \tag{S21}$$

We emphasize that for the *centered* interaction $(n_i - \tfrac{1}{2})(n_j - \tfrac{1}{2})$ no additional constant terms appear.

Hubbard model

The Hubbard Hamiltonian in the main text reads

$$H_{\text{Hub}} = -t_{\text{hop}} \sum_{\langle i,j \rangle, \sigma} \left(c_{i\sigma}^\dagger c_{j\sigma} + \text{H.c.} \right) + V \sum_i \left(n_{i\uparrow} - \tfrac{1}{2} \right) \left(n_{i\downarrow} - \tfrac{1}{2} \right). \tag{S22}$$

Using Eqs. (S17) and (S19), we obtain

$$H_{\text{Hub}} = -\frac{i\,t_{\text{hop}}}{2} \sum_{\langle i,j \rangle, \sigma} \left(\gamma_{2i-1,\sigma}\gamma_{2j,\sigma} - \gamma_{2i,\sigma}\gamma_{2j-1,\sigma} \right) - \frac{V}{4} \sum_i \gamma_{2i-1,\uparrow}\gamma_{2i,\uparrow}\gamma_{2i-1,\downarrow}\gamma_{2i,\downarrow}. \tag{S23}$$

Total current operator

The total current along a fixed lattice direction $\hat{x}$ is

$$J = -it_{\text{hop}} \sum_{i,\sigma} \left(c_{i\sigma}^\dagger c_{i+\hat{x},\sigma} - c_{i+\hat{x},\sigma}^\dagger c_{i\sigma} \right). \tag{S24}$$

Using Eq. (S18) we obtain its Majorana representation

$$J = -\frac{it_{\text{hop}}}{2} \sum_{i,\sigma} \left(\gamma_{2i-1,\sigma}\gamma_{2(i+\hat{x})-1,\sigma} + \gamma_{2i,\sigma}\gamma_{2(i+\hat{x}),\sigma} \right). \tag{S25}$$

RELATION BETWEEN MOMENTS AND LANCZOS COEFFICIENTS

This relation is well-known [1, 2]. First one defines determinants of Hankel matrices of moments,

$$h_n = \begin{vmatrix} \mu_0 & \mu_1 & \mu_2 & \cdots & \mu_n \\ \mu_1 & \mu_2 & \mu_3 & \cdots & \mu_{n+1} \\ \vdots & \vdots & \vdots & \ddots & \vdots \\ \mu_n & \mu_{n+1} & \mu_{n+2} & \cdots & \mu_{2n} \end{vmatrix}. \tag{S26}$$

Here odd moments should be put to zero.

The relation then reads

$$\begin{aligned} b_1^2 &= h_1, \\ b_2^2 &= \frac{h_2}{h_1^2}, \\ b_n^2 &= \frac{h_{n-2}\,h_n}{h_{n-1}^2} \quad \text{for} \ \ n \geq 3. \end{aligned} \tag{S27}$$

From computational perspective, it is convenient to use these relations to get Lanczos coefficients from moments. This way one avoids explicitly constructing the Lanczos basis – a procedure that would incur a considerable RAM overhead.

TRANSPORT PROPERTIES BY RECURSION METHOD

Computing diffusion constant

In the case of infinite temperature, $\beta = 0$, and half-filling, $\langle n_{i\sigma} \rangle_\beta = 1/2$, thermal averaging reduces to normalized tracing:

$$\langle A \rangle_{\beta=0} = \text{tr}A/\text{tr}\mathbb{1}. \tag{S28}$$
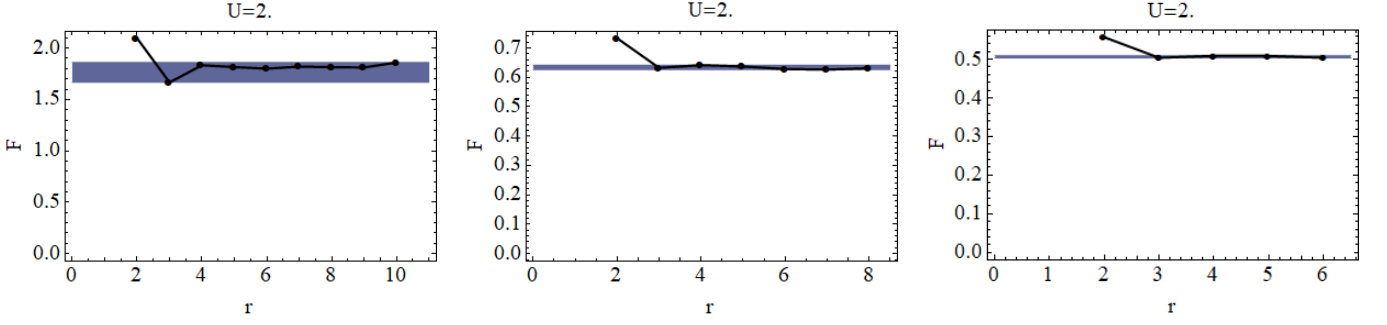
FIG. S1. Sequence of F_r for the 2D Hubbard model (first plot), 2D t-V model (second plot) and 3D t-V model (third plot). The interaction strength is $V = 2$. The uncertainty estimate is shown as a blue horizontal stripe.

In what follows we omit subscript β in $\langle\ldots\rangle_\beta$.

One can rewrite the definition of $C(t)$ using this thermal average:

$$C(t) \equiv \frac{\text{tr}[J(t)J]}{\text{tr } J^2} = \frac{\langle J(t)J\rangle}{\langle J^2\rangle}. \tag{S29}$$

As explained in the main text, $D = \delta N_{\text{tot}}^{-2} \operatorname{Re} \int_0^\infty dt \langle J(t)J\rangle_\beta$. This can be rewritten using eq.(S29):

$$D = \frac{\langle J^2\rangle}{N_{\text{tot}}^2} \int_0^\infty dt\, C(t). \tag{S30}$$

One easily finds that in the t-V and Hubbard models the prefactor in the above formula reads

$$\frac{\langle J^2\rangle}{N_{\text{tot}}^2} = 2. \tag{S31}$$

The hard part is computing $F \equiv \int_0^\infty dt\, C(t)$. Following [3], we approximate F by F_r, where

$$F_r = \frac{1}{b_r} \prod_{m=1}^{[r/2]} \frac{b_{2m}^2}{b_{2m-1}^2} \times \begin{cases} 1/p_r & \text{for even } r, \\ p_r & \text{for odd } r, \end{cases} \tag{S32}$$

$[r/2]$ is the integer value of $(r/2)$ and

$$p_r = \Gamma\left(\frac{r}{2} + \frac{\gamma}{2\alpha}\right) \Gamma\left(\frac{r}{2} + \frac{\gamma}{2\alpha} + 1\right) \bigg/ \left(\Gamma\left(\frac{r}{2} + \frac{\gamma}{2\alpha} + \frac{1}{2}\right)\right)^2. \tag{S33}$$

In principle, the sequence of F_r converges to F in the limit of $r \to \infty$ [3, 4]. In practice, one can approximate F by F_r at a finite r whenever the convergence is fast. If $n_{\max}$ Lanczos coefficients b_n are available, one can compute F_2, F_3,...,$F_{n_{\max}}$. The sequences F_r for different models and interaction strengths are shown in Fig. S1. One can see that the sequence reasonably converges already for moderate available values of $n_{\max}$.

To estimate the uncertainty of our procedure, we drop the first value of the sequence, F_2, and assume that the true value of F lies between the maximal and minimal values of the remaining sequence, see Fig. S1.

Comparison to the perturbative result

Ref. [5] reports a perturbative result for the dc conductivity of the 2D Hubbard model at $T = 4$ (in our units). Thanks to the Nernst-Einstein relation, dc conductivity can be converted to the diffusion constant. If one assumes the linear scaling of the dc conductivity with temperature at high temperatures, see eq. (9) in the main text, the result of [5] implies the infinite-temperature diffusion constant $D = 12.54/V^2$. Fit to our data at small V gives a very close result, $D = 12.84/V^2$.

* ermakov1054@yandex.ru

† lychkovskiy@gmail.com

[1] M. Dupuis, Progress of Theoretical Physics **37**, 502 (1967).

[2] V. Viswanath and G. Müller, *The recursion method: application to many-body dynamics* (Springer, 1994).

[3] J. Wang, M. H. Lamann, R. Steinigeweg, and J. Gemmer, Phys. Rev. B **110**, 104413 (2024).

[4] C. Joslin and C. Gray, Molecular Physics **58**, 789 (1986).

[5] J. Kovačević, M. Ferrero, and J. c. v. Vučičević, Phys. Rev. Lett. **135**, 016502 (2025).